Proceedings World Geothermal Congress 2010
Bali, Indonesia, 25-29 April 2010

Corrosion and Scaling in High Gas (25wt%) Geothermal Fluids

Keith A Lichti[1] and Rosalind H. Julian[1]

[1]Quest Integrity Ltd., PO Box 38 096, Lower Hutt 5045, New Zealand

k.kichti@questintegrity.com, r.julian@questintegrity.com

Keywords: high gas, geothermal, corrosion, carbon steel, on-line, monitoring, electrical resistance, coupons

ABSTRACT

The majority of New Zealand geothermal resources produce separated steam with moderate gas content, 3 to 5 wt%, with these gases being predominantly CO_2 but with significant concentrations of H_2S and NH_3. The ratios of these gases are relatively constant in the New Zealand fields giving near neutral to alkali chloride waters. Corrosion in the moderate gas geothermal fields has been extensively studied. Corrosion behaviour in high gas geothermal fields such as at Ngawha having up to 10 wt% gas was initially predicted to be equally low and acceptable as for moderate gas fields. This paper describes work aimed at determining the corrosivity of a high gas geothermal fluid. A mobile corrosion test facility, developed in house, was used to measure the corrosion rates of three common construction materials; a carbon steel, a 12% Cr stainless steel and 316 stainless steel in a high gas geothermal fluid. The tests were completed by mixing gas separated from Broadlands/Ohaaki Well BR3 into Well BR22 two-phase produced fluid to give a total gas content in separated steam of 25 +/- 5 wt%. The measured corrosion rates in separated water and separated steam were low and acceptable and comparable to those in fluids having more moderate gas concentrations. In two phase fluid the test results showed sensitivity to erosion corrosion.

1. INTRODUCTION

Corrosion properties of fluids derived from production wells of geothermal fields in the Taupo Volcanic Zone (TVZ) of New Zealand have been extensively studied; see Table 1. The produced fluids are near neutral to alkali chloride waters, with relatively low chloride concentration and have gas concentrations ranging from 0.1 wt% to 4.6 wt%. The Ngawha geothermal field in Northland, well outside the TVZ, has a higher gas content, up to 10 wt%.

The corrosion studies completed for the geothermal fields in the TVZ demonstrated a change in corrosion product stability from the low gas field of Wairakei, 0.1wt% gas, to the higher gas fields of Broadlands/Ohaaki and Kawerau, 2 to 5 wt% gas. These corrosion products are important as they form a physical barrier between the exposed metal and the corrosive environment. On carbon steels, magnetite stability dominated at Wairakei field while the higher gas systems showed a predominance of iron sulfides. However, in many instances the sulfides overlaid a thin layer of magnetite, Borshevesky *et al.* (1982). It was argued that the moderate gas geothermal systems stabilised iron sulfides that gradually formed and blocked the surface from the corrosive environment. This gave a lower partial pressure of H_2S near the surface that allowed stability of magnetite. These results suggested that a high gas geothermal fluid would also form stable protective films and give low corrosion rates (Wilson and Lichti, 1983).

Although from thermodynamic considerations, a low corrosion rate was predicted for the high gas fluids, these predictions required confirmation. This was especially so because of the tendency to pitting corrosion noted in previous studies, even with low gas concentrations, Lichti *et al.* (1981). Measurement of corrosion properties of fluids with gas content greater than that observed for the Ngawha geothermal field was proposed in order to reliably select materials for the full range of New Zealand geothermal fluid chemistries. Work was completed on corrosion monitoring of high gas geothermal fluids using a mobile corrosion test facility with short term on-line corrosion monitors and ASTM coupons in 1985. Lichti *et al*. (1986) described the test facility and demonstrated that similar results could be obtained from the vertically oriented test vessels *vs.* the horizontal vessels used previously at Broadlands/Ohaaki well BR22.

This paper gives results for common construction materials exposed to a high gas geothermal fluid and compares these results with an existing database from moderate gas tests.

Table 1 Separated steam gas chemistries of some New Zealand geothermal fields.

Field	Well	Date	CO2	H2S	NH3	H2	Residual	Gas in Steam	Corrosion Testing
			mmol/100 mol steam					wt%	
Wairakei	HP Steam		39.1	2.39	0.50	0.25	n/a	0.1	Marshall and Braithwaite, 1973, Lichti and Bacon, 1998 Soylezemoglu *et al.*, 1980
Broadlands/ Ohaaki	BR22	1985	841	17.6	5.4	0.79	16.2	2.1	Braithwaite and Lichti, 1981 Lichti and Wilson, 1983, Lichti *et al.*, 1981, Lichti *et al.*, 1985
Kawerau	KA21	1995	1797	34	3.65	3.55	83.7	4.6	Lichti *et al.*, 1997
Mokai	MK3	1982	309	13.3	0.18	0.77	14.2	0.8	Chemistry data from Plum and Henley, 1983
Rotokawa	RK4	1984	925	21.6	6.4	6.20	40.7	2.4	Chemistry data from Henley and Middendorf, 1985
Ngawha	NG9	1980	2825	35.2	34.0	7.60	79.3	7.3	Chemistry data Sheppard, 1980, Wilson and Lichti, 1983

2. Corrosion Testing

The majority of the high gas tests were conducted in continuously flowing refreshed environments with one test in a high flow two-phase fluid of unknown velocity, Lichti *et al*. (1991).

The three construction materials tested were:

- Carbon steel, G10180.
- 12% Cr stainless steel, S41000.
- stainless steel, S31600

The geothermal fluids tested included:

- Two-phase fluid at 185ºC under high flow and at 170ºC under low flow conditions.
- Separated Water at 150ºC under low flow conditions.
- Separated Steam at 160ºC under low flow conditions.

A schematic of the test arrangement is shown in Figure 1. The tests were completed by mixing gas separated from Broadlands/Ohaaki Well BR3 into Well BR22 two-phase produced fluid to give a total gas content in separated steam of 25 +/- 5 wt%. The high flow two-phase fluid was tested in a 32 mm vertical pipeline with the flow upward. The two-phase test fluid was allowed to separate and steam and water were remixed before entering the vessel. A 10" vertical separator and surge tank were used to separate the high gas steam and brine. The separated water was in a near horizontal flanged 100 mm diameter vessel with bottom of flange entry and top of flange exit to avoid formation of a gas pocket. The two phase fluid and separated steam were tested in vertical vessels with flow from the top to the bottom.
Figures 2 and 3 illustrate the vessels and side port entry points for on-line monitors. Coupons were inserted into the flanged vessels for two-phase fluid, separated water and separated steam. Electrical resistance probes were inserted into side ports of all test pipes and vessels.

2.1 Exposure Conditions

The separated water and separated steam were sampled and the chemistry of each measured, Glover (1986). These chemistries were combined using the programme "WATCH", Arnorsson *et.al.* (1982), Arnorsson and Bjarnason (1993), to a single phase condition at 295ºC and boiled to 185ºC, 170ºC and 150ºC to give the high temperature chemistry of the two-phase fluids and separated water. The as-analysed steam chemistry was used to calculate the high temperature chemistry of the steam condensate using the method of Glover (1982). The high temperature chemistries are summarised in Table 2.

2.2 Corrosion Monitors

ASTM weight loss coupons (ASTM G1 - 03 and G4 - 95 (2008)) and electrical resistance (ER) probes (now described in ASTM G96 - 90 (2008)), Figure 4, were employed to obtain corrosion data for the short term test. Figure 4 shows a fully welded 100 mm long finger type Corrosometer™ probe of carbon steel, a 50 mm long finger type probe of S31600 and a hairpin type probe of S41000.

Braithwaite and Lichti (1981) describe the method of cleaning that was used to remove the corrosion products and scales . Pitting propensity was measured with reference to ASTM G46 – 2005. Collected corrosion products were analysed by X-Ray Diffraction.

™ Rohrback Cosascco Systems

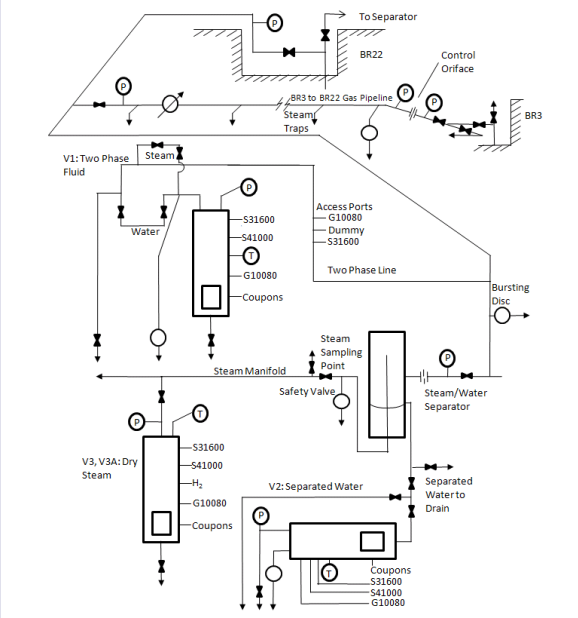

Figure 1. Schematic of mobile corrosion test facility.

Table 2: High temperature chemistries of test fluids.

	2 Phase	2 Phase	Water	Steam
Temperature ºC	**185**	**170**	**150**	
Enthalpy kJ/kg	**1323**	**1323**	**1323**	
pH	**6.34**	**6.42**	**6.54**	**6.11**
Vapour Frac.	**0.268**	**0.2934**	**Water**	**Steam**
Units	mol/kg	mol/kg	mol/kg	mol/kg
CO_2	--	--	--	5.41E-03
H_2CO_3	1.18E-02	7.59E-03	4.26E-03	--
HCO_3^-	3.48E-03	3.64E-03	3.87E-03	1.03E-03
CO_3^{--}	4.29E-07	6.90E-07	1.29E-06	--
Total C	**1.53E-02**	**1.12E-02**	**8.13E-03**	**1.03E-03**
H_2S	3.20E-04	2.05E-04	1.14E-04	1.77E-04
HS^-	1.33E-04	1.26E-04	1.14E-04	3.22E-05
HSO_4^-	1.29E-07	6.82E-08	2.84E-08	--
SO_4^{--}	3.48E-05	3.70E-05	3.99E-05	--
Total S	**4.88E-04**	**3.68E-04**	**2.67E-04**	**2.09E-04**
NH_3	--	--	--	5.79E-04
NH_4OH	4.57E-04	3.94E-04	3.25E-04	--
NH_4^+	2.70E-04	3.20E-04	4.03E-04	1.06E-03
Total N	**7.27E-04**	**7.13E-04**	**7.28E-04**	**1.06E-03**
Cl^-	3.14E-02	3.25E-02	3.41E-02	--
Total Cl	**3.14E-02**	**3.25E-02**	**3.41E-02**	--
H_4SiO_4	8.95E-03	9.27E-03	9.68E-03	--
$H_3SiO_4^-$	4.14E-05	5.38E-05	7.31E-05	--
$H_2SiO_4^{--}$	1.67E-09	2.92E-09	5.71E-09	--
Total Si	**9.00E-03**	**9.32E-03**	**9.76E-03**	--
H_3BO_3	2.99E-03	3.08E-03	3.23E-03	--
H_2BO_3	9.66E-06	1.26E-05	1.79E-05	--
Total B	**3.00E-03**	**3.10E-03**	**3.25E-03**	--
Ca^{++}	2.12E-05	2.41E-05	2.81E-05	--
Total Ca	**2.12E-05**	**2.41E-05**	**2.81E-05**	--
Fe^{++}	1.12E-06	3.04E-06	5.09E-06	--
Fe^{+++}	1.10E-21	2.11E-21	2.10E-21	--
$Fe(OH)_3$	2.65E-06	1.14E-06	1.71E-07	--
$Fe(OH)_4^-$	3.25E-06	1.31E-06	1.79E-07	--
Total Fe	**7.03E-06**	**5.49E-06**	**5.44E-06**	**1.00E-05**
Mg^{++}	1.22E-06	1.27E-06	1.35E-06	--
Total Mg	**1.22E-06**	**1.27E-06**	**1.35E-06**	--
K^+	3.75E-03	3.89E-03	4.08E-03	--
Total K	**3.75E-03**	**3.89E-03**	**4.08E-03**	--
Na^+	2.98E-02	3.09E-02	3.24E-02	--
Total Na	**2.98E-02**	**3.09E-02**	**3.24E-02**	--
pp H_2 (atm)	**4.28E-03**	**2.76E-03**	**1.49E-03**	**1.80E-04**
Calcite SI	**-0.724**	**-0.778**	**-0.843**	--
SiO_2 SI	**-0.194**	**-0.125**	**-0.028**	--

Figure 2. Test vessels for steam, V3 and two-phase fluid, V1.

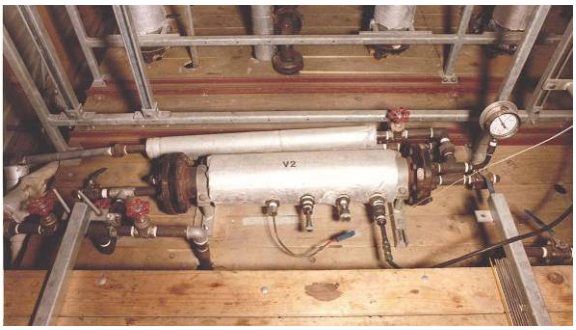

Figure 3. Separated water test vessel, V2.

Figure 4. Corrosion monitors used in high gas trials, two-phase fluid, V1.

2.2.3 Weight Loss coupons

Corrosion rate was established by measuring loss in weight over time of ASTM G1 - 03 type coupons. The following formula was used:

$$ML = \frac{\delta}{\rho A} \times 10^3 \qquad (1)$$

ML: material loss (μm) (obtained by controlled removal of scales and corrosion products),

δ : weight loss (mg),

ρ : density of test material (mg/mm^3)

A: exposed area of test material (mm^2),and:

$$CR = \frac{ML \times const}{t} \qquad (2)$$

CR: corrosion rate (μm.year^{-1}),
const: 31.557 x 10^6 (number of seconds per mean solar year),
t: duration of exposure period (s), respectively.

2.2.1 Electrical Resistance Probes

"Corrosometer^{TM}" ER probes, ASTM G 96 - 90 (1996) were used to provide continuous corrosion rates for the duration of the experiment. These probes have good sensitivity to variations in conditions within a system, Lichti and Soylemezoglu (1979).

The "Corrosometer^{TM}" consists of a probe inserted through an access port, connecting to a cable and a meter. It operates by measuring the electrical resistance of the exposed test element of the probe. As the cross sectional area of the probe is reduced by corrosion the electrical resistance is increased. The resistance of the probe is compared to an internal reference element to compensate for small temperature variations. The corrosion rate can be determined according to the following relationship:

Material loss (mils/year) =
ΔDial reading x probe multiplier (3)

Corrosion rate (mils/year) =
ΔDial reading/Time (days) x 0.365 x probe multiplier (4)

Where a mil is one thousandth of an inch and the multiplier depends on the dimensions of the probe used.

An automated 15 channel Corrosometer^{TM} Rohrback Model 4100 and single channel portable Rohrback Model CK3 were used to measure change in dial readings to 0.5.

3. RESULTS

Exposure tests were run for periods of up to 5.7 weeks. The end time was selected to give sufficient results from on-line monitors to determine the corrosion kinetics for each test; linear, parabolic, logarithmic or other.

3.1 Two-Phase Fluids

This test ran for 5.7 weeks as the monitors were exposed to high velocity two-phase fluid for the full duration of the test. The monitors were analysed and cleaned to reveal the underlying corroded surfaces. Table 3 shows corrosion results obtained. The probes and coupons had deposits of silica but the carbon steels also showed crystalline iron containing compounds. The carbon steel rod coupon and Corrosometer^{TM} had pyrrhotite ($Fe_{(1-x)}S$) and mackinawaite ($Fe_{(1+x)}S$) corrosion products, Table 3. Cleaned surfaces showed localised pitting corrosion, even on the stainless steels, with the maximum pit depth being 43 μm on the S41000 ER probe. A linear corrosion rate was indicated for the carbon steel by the on-line ER probe results, Figure 5, but the rate was low at 0.05 mm/year.

Table 3. Two-Phase Fluid at 185ºC after 5.7 weeks.

Material	-Monitor Type	Exposure Time (Weeks)	Scaling Details Type/ Thickness	Material Loss (µm)	Material Loss/ Corrosion Rate	Corrosion Type	Pitting Details Density Depth Mean(max) µm(µm)
Carbon Steel	-Rod Coupon (E-1)	5.7	SiO2 + Crystalline/ Variable and Rough	7.37	5.16 µm(4w)-1 67.2 µmy-1	N(R)-PE	P(A5) 18(32)
	-Corrosometer (PR1-Aug81-13)	5.7	SiO2 + Crystalline/ Variable and Rough	5.69	3.99 µm(4w)-1 51.9 µmy-1	N(R)-PE	P(A5) 20(43)
S31600	-Corrosometer (MPR18-316-7)	5.7	SiO2/ Variable and Rough	Not Detected	Not Detected Not Detected	U-P	P(<A1) 10(20)

Note: Carbon Steel Rod Coupon and Corrosometer ™ shown to have Pyrrhotite ($Fe_{(1+x)}S$)and Mackinawaite ($Fe_{(1-x)}S$).

Table 4. Separated water at 150ºC after 4.57 weeks.

Material	-Monitor Type	Exposure Time (Weeks)	Scaling Details	Material Loss (µm)	Material Loss/ Corrosion Rate	Corrosion Type	Pitting Details Density Depth Mean (Max) µm (µm)
Carbon Steel	-Coupons (R2-77)	4.57	SiO_2/ 5.9±3.0 7.2(Wt Gain)	0.652	0.571 µm(4w)$^{-1}$ 7.44 µmy^{-1}	U-PC	P(A5) 14(27) C(A5) 24(60)
	-Corrosometer (PR3A+MPR27-S83-2)	4.57	SiO_2 +/ Variable + Corrosion Product	1.143	(1.14) µm(4w)$^{-1}$ (1.15) µmy^{-1}	N-PC	P(A5) 148(429)* C(A4) –(130)
S41000	-Coupon (R2-17-410)	4.57	SiO_2/ 4.0±2.0 5.07(Wt Gain)	0.434	0.380 µm(4w)$^{-1}$ 4.95 µmy^{-1}	U-PC	P(A1) 14(30) C(A5 26(37)
	-Corrosometer (MPR19-p38)	4.57	SiO_2/ SiO_2 =5.6±1.6 Corrosion Products	Not Detected	Not Detected	U	Not Detected
S31600	-Coupons (R2-19-316L)	4.57	SiO_2/ 3.4±1.4. 4.84(Wt Gain)	0.078	0.068 µm(4w)$^{-1}$ 1.01 µmy^{-1}	U	Not Detected
	-Corrosometer (MPR20-316-2)	4.57	SiO_2/ Variable and Nodular: Top=5 Side=Nil Bottom=3	Not Detected	Not Detected	U	Not Detected

Note: Carbon Steel Coupons had Mackinawaite and amorphous material in major concentrations plus Troilite (FeS) and Pyrrhotite.

Table 5. Separated steam at 170ºC after 5 weeks.

Material	-Monitor Type	Exposure Time (Weeks)	Scaling Details Type/ Thickness	Material Loss (µm)	Material Loss/ Corrosion Rate	Corrosion Type	Pitting Details Density Depth Mean (Max) µm (µm)
Carbon Steel	-Coupons (R3-77)	5	Crystalline/ Thin Adherent	4.86	3.89 µm(4w)$^{-1}$ 50.7 µmy^{-1}	U(R)-PC	P(A5) 20(34) C(A5) 10(17)
	-Corrosometer (PR4 -S83-3)	5	Crystalline/ Thin Adherent	1.45	(1.30) µm(4w)$^{-1}$ (6.6) µmy^{-1}	U(R)-P	P(A3) 15(32)
S41000	-Coupon (R3-17-410)	5	Crystalline/ Thin Adherent	2.13	(0.910) µm(4w)$^{-1}$ (4.32) µmy^{-1}	U-PC	P(A3) 19(55) C(A1) 22(58)
	-Corrosometer (PR14-P40)	5	Crystalline/ Thin Adherent	0.965	0.65 µm(4w)$^{-1}$ 7.2 µmy^{-1}	U	Not Significant (micropitting all <5µm)
S31600	-Coupons (R3-19-316L)	5	Thin Interference Films	0.149	0.119 µm(4w)$^{-1}$ 1.55 µmy^{-1}	U	Not Detected
	-Corrosometer (PR5+MPR21-316-3)	5	Thin Interference Films	Not Detected	Not Detected	U-P	P(<A1) –(54)

Note: Carbon Steel Coupons had Troilite and Pyrrhotite corrosion products.

Note that in Tables 3 to 5: N=Non-uniform Corrosion, U=Uniform Corrosion, R=Rough Corrosion Surface, P=Pitting Corrosion, C=Crevice Corrosion, A1 to A5 represent density of pitting corrosion from smallest to largest from ASTM G46 – 2005.

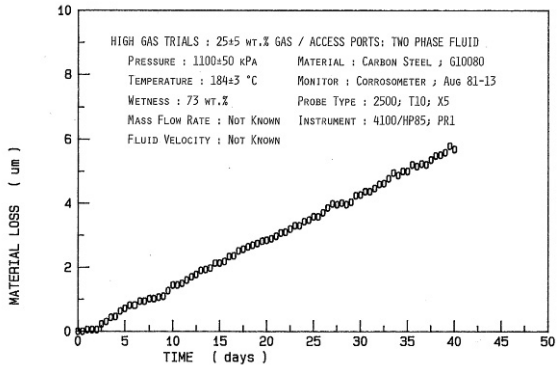

Figure 5. ER probe result for carbon steel in high velocity two-phase fluid.

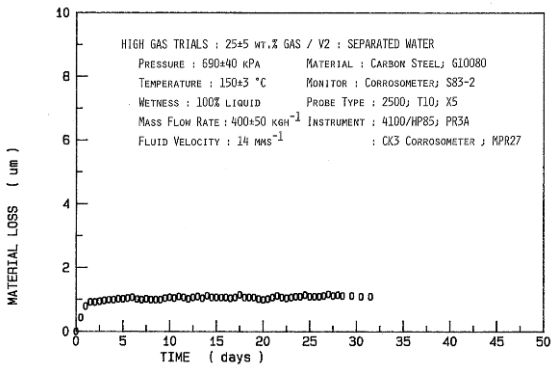

Figure 6. ER probe result for carbon steel in separated water.

The onset of erosion in the high flow test section was not comparable to test results under lower gas conditions and no flow monitor was available to calibrate the test, so the reason for the onset of erosion remains unresolved.

The lower temperature, 168ºC, two-phase fluid had a known fluid velocity of 400 kg/hr of 86% water through the 100 mm diameter vessel. All of the monitors were readily scaled with silica after the 5 week test and low corrosion rates were measured, 0.2 to 12 µm/year. All of the monitors exhibited local corrosion pits but the depth of these was a maximum of 44 µm on the S41000 alloy.

3.2 Separated Water

This test ran for 4.57 weeks in the horizontal vessel filled with low velocity separated water; mass flow of 400 kg/hour. The carbon steel ER probe exhibited logarithmic kinetics, Figure 6. All of the exposed monitors exhibited a layer of silica on completion of the test, typically of the order 5 µm thick, however the monitors showed excess iron corrosion products on most surfaces and a tendency to air oxidation on drying indicating poor control of corrosion, Figure 7. Carbon steel coupons had mackinawaite and amorphous material in major concentrations plus troilite (FeS) and pyrrhotite ($Fe_{(1-x)}S$) corrosion products. Removal of the silica layer and corrosion products showed localised pitting corrosion on carbon steel and S41000 but not on S31600. Corrosion rates decreased in the order carbon steel, S41000, S31600, the highest rate being 7.4 µm/year applying linear kinetics, Table 4. The absence of a coherent layer of silica on carbon steel probes that completely limited corrosion product formation was not seen in moderate and low gas fluids, Lichti *et al.* (2000).

3.3 Separated Steam

This test ran for 5 weeks as the monitors were exposed to low velocity saturated stream at a mass flow of 50 kg/hour. The carbon steel coupons had a mixture of troilite (FeS) and pyrrhotite corrosion products. The exposed monitors were analysed and cleaned to reveal the underlying corroded surfaces. Table 5 shows corrosion results obtained. The carbon steel and S41000 probes and coupons had crystalline corrosion products while the stainless steel S31600 exhibited thin interference films. The density of pitting decreased as the alloy content increased, but even the stainless alloy was susceptible to localised corrosion at near the maximum depth of all the monitors tested, 54 µm. Parabolic kinetics were indicated by the carbon steel on-line monitor, Figure 8, while the S41000 alloy showed a linear rate of corrosion, at a very low level, Figure 9.

Figure 7. Corrosion monitors used in high gas trials, separated water, V2.

4. COMPARISON WITH HISTORICAL RESULTS

4.1 Corrosion properties

Results obtained in vertical test vessels during commissioning of the Mobile Corrosion Test Facility were initially compared with those obtained previously in horizontal vessels, Lichti *et al.* (1985). These comparisons indicated good reproducibility and provided confidence that the high gas results could be readily compared with the existing database of corrosion results; see for example Braithwaite and Lichti (1981) and Lichti *et al.* (1981). The corrosion kinetics, the magnitude of the corrosion and the pitting characteristics are summarised in Table 6. This table also includes a summary of the high gas results presented in Tables 3 to 5. All of the results are normalised to 4 weeks which was the shortest exposure time used for the historical results obtained in horizontal vessels.

Table 6 shows a common set of kinetics for both moderate and high gas tests in the low flow two-phase and separated stream test vessel environments where parabolic and logarithmic corrosion kinetics were observed. The exceptions were:

- Separated water in the low gas tests showed deposition of amorphous silica at low and acceptable levels, of the order 0.24 mm/year, whereas the high gas tests showed limited adherent silica scale formation with non-protective corrosion products forming over large areas.

- The new test in high velocity two-phase flow resulted in a linear rate of corrosion although the rate was relatively low at 0.05 to 0.07 mm/year.

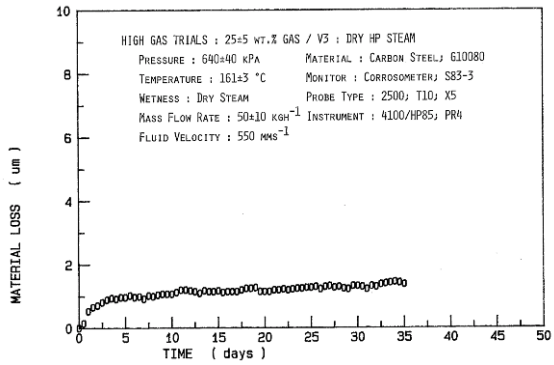

Figure 8. ER probe result for carbon steel in separated steam.

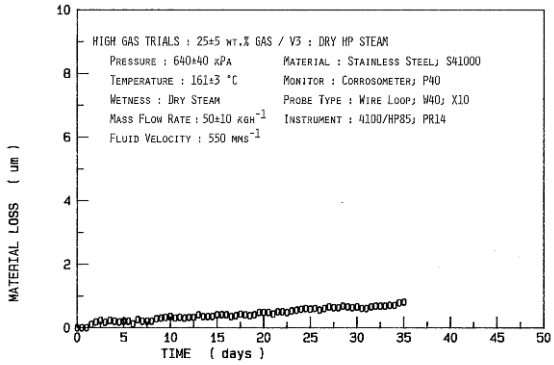

Figure 9. ER probe results for S41000 in separated steam.

4.2 Corrosion Thermodynamics

The corrosion product stability can be described using potential-pH type Pourbaix diagrams that model thermodynamic properties for specific corrosion reactions, Chen *et.al.* (1983). The principal reactions considered by the equilibrium phase diagrams for formation of iron sulfide and iron oxide corrosion products, in solutions having H_2S include:

$$3Fe + 4H_2O \rightarrow Fe_3O_4 + 8H^+ + 5e^- \quad (5)$$

$$3Fe^{2+} + 4H_2O \rightarrow Fe_3O_4 + 8H^+ + 2e^- \quad (6)$$

$$Fe + H_2S \rightarrow FeS + 2H^+ + 2e^- \quad (7)$$

$$Fe^{2+} + H_2S \rightarrow FeS + 2H^+ \quad (8)$$

$$Fe^{2+} + 2H_2S \rightarrow FeS_2 + 4H^+ + 2e^- \quad (9)$$

$$FeS + H_2S \rightarrow FeS_2 + 2H^+ + 2e^- \quad (10)$$

The formation of stable passive films, such as magnetite Fe_3O_4, pyrrhotite $Fe_{(1-x)}S$ and pyrite FeS_2 on carbon and low alloy steels in geothermal fluids is dependent on the chemical composition of the condensate in equilibrium with the steam, and on the kinetics of formation of the various compounds:

- Total S concentration determines the relative stability of iron-based corrosion product (Fe_3O_4) or (FeS).
- The ratio of carbon dioxide to ammonia (CO_2/NH_3) determines the pH, provided the hydrogen chloride or sulfur dioxide contents of the steam are low and the partial pressure of oxygen is low.

Table 6: Comparison of moderate and high gas fluid corrosion results.

Test Results for Broadlands Well BR22 at 2.5wt% Gas; G10180, S41000 and S31600				
Environment	**Corrosion and Scaling Products**	**Corrosion Kinetics**	**Form of Corrosion**	**Pitting Details**
-Material	**A=Adherent F=Flaking**	**Estimated Type (µm at 4 weeks)**	**U=Uniform P=Pitting C=Crevice R=Rough Surface**	**To 4 Weeks Density* Depth Mean(max) µm(µm)**
V1: Two Phase Fluid				
MTCF-Carbon Steel	Silica + Sulfides (A)	Logarithmic (<0.5)	U-P	P(A3) 17(44)
Old Rig-Carbon Steel	Sulfides + Oxides (A)	Logarithmic (<7.0)	U-PC	P(A4) 18(29)
-S41000	Sulfides (+ Oxides) + Silica (A)	Parabolic (Linear After Shutdown) (<5)	U-PC	P(A2) 19(29)
-S31600	Thin Interference Films + Silica	Logarithmic(<0.1)	U-PC	P(A1) 32(43)
V2: Separated Water				
MTCF-Carbon Steel	Silica (A)	Logarithmic (<1.0)	U-P	P(A3) 22(32)
Old Rig-Carbon Steel	Silica + Sulfides (A)	Logarithmic (<0.5)	U-P	P(A1) -(<5)
-S41000	Silica + Sulfides (A)	Logarithmic (<0.5)	U	Not Analysed
-S31600	Silica (A)	Logarithmic (<0.1)	U	Not Analysed
V3: Dry HP Steam				
MTCF-Carbon Steel	Sulfides (+ Oxides) (A)	Parabolic (<3.5)	U-P	P(A5) 5(12)
Old Rig-Carbon Steel	Sulfides (+ Oxides) (A)	Parabolic (<10/0)	U-PC	P(A5) 24(46)
-S41000	Sulfides (+ Oxides) (A/F)	Parabolic (Linear After Shutdown) (<50.0)	U-PC	P(A2) 20(71)
-S31600	Thin Interference Films (A)	Logarithmic(<0.1)	U	Not Analysed
Estimate of High Gas Corrosion Kinetics for Carbon Steel, S41000 and S31600				
Access Ports: Two Phase Line				
-Carbon Steel	Silica + Sulfides (F)	Linear(4.0)	N (R) –PE	P(A5) 19(43)
-S31600	Silica (A/F)	Logarithmic (nil)	U-P	P(<A1) 10(44)
V1: Two Phase Fluid				
-Carbon Steel	Silica (A)	Logarithmic (0.2)	U-PC	P(A5) 10(44)
-S41000	Silica (A)	Logarithmic (1.0)	U-PC	P(A1) 20(40)
-S31600	Silica (A)	Logarithmic (0.02)	U-PC	Not Detected
V2: Separated Water				
-Carbon Steel	Silica + Sulfides (F)	Logarithmic (1.2) (+ Standyby Corrosion)	U-PC N-PC)	P(A5) 19(60) P(A5) 148 (429)
-S41000	Silica + Sulfides (F)	Logarithmic (0.4)	U-PC	P(A3) 20(37)
-S31600	Silica (A)	Logarithmic (0.08)	U	Not Detected
V3: Dry HP Steam				
-Carbon Steel	Sulfides (+ Oxides) (A)	Parabolic (4.0)	U (R) –PC	P(A5) 18(35)
-S41000	Sulfides (+ Oxides) (A)	Linear (1.7)	U-PC	P(A2) 21(58)
-S31600	Thin Interference Films (A)	Logarithmic (0.12)	U-P	P(<A1) –(54)

- In the reducing environment (negligible oxygen), common to geothermal fluids, the corrosion potential remains at or below the hydrogen evolution line in the potential-pH diagrams.

High gas Pourbaix diagrams for two-phase fluid at 185°C and for separated steam at 160°C, Figures 10 and 11, were prepare to allow comparison with those for moderate and low gas environments, see Figures 12 and 13.

The diagrams progress from magnetite stability predicted and observed under low gas conditions, as at Wairakei, to sulfide stability predicted and observed at moderate gas content, as at Broadlands/Ohaaki. In addition, the moderate gas content fluids are known to promote formation of a thin layer of magnetite under the formed sulfide scales, Lichti *et al.* (1997). The similar corrosion rates in low and moderate gas geothermal systems has been attributed to the formation of this thin magnetite layer. The potential-pH diagrams show that the high gas geothermal fluids are similar to moderate gas fluids and the measured corrosion rates for the two systems were very similar, Table 6. The readily collected sulfide scales present on carbon steel exposed in the two systems were similar. Cross sections of exposed high gas materials were not prepared at the time of analysis, however it is expected that a thin layer of magnetite will be present under the formed sulfide scales of the high gas exposed monitors, Lichti *et al.* (2003).

The tests conducted do not give clear indication of the reason for the onset of erosion corrosion in the high velocity two-phase fluid, although the temperature and flow rates were the highest tested.

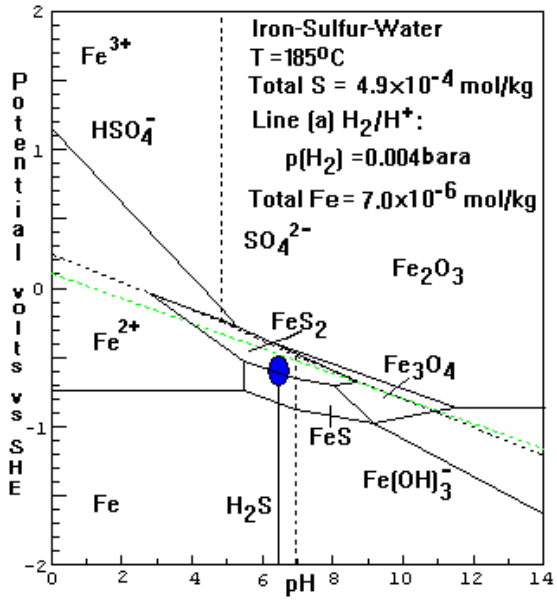

Figure 10. High Gas Pourbaix diagram for two phase fluid at 185°C.

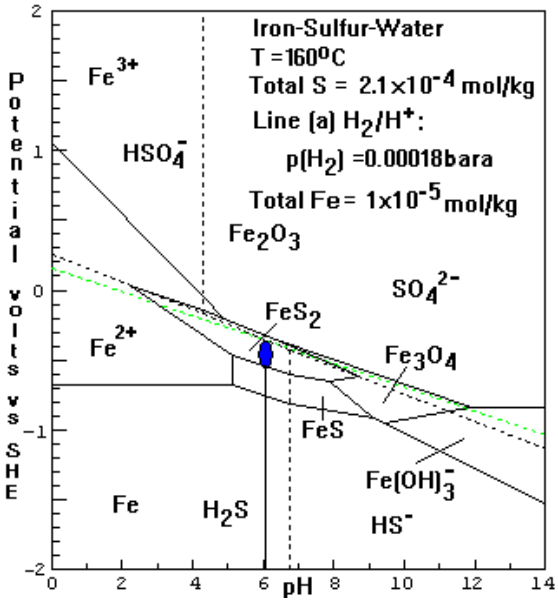

Figure 11 High Gas Pourbaix diagram for steam at 160°C.

4. CONCLUSIONS

The results obtained showed that:

1. Onset of erosion-corrosion was observed in the two-phase fluid tested under high gas conditions. The reason for this has not been resolved, however it coincided with the highest temperature tested and the highest flow rate tested.

2. Silica scales formed on carbon steel and S41000 in separated water tested during the high gas trials were not uniform and significant corrosion product formed over locally corroded areas. In addition the test showed greater sensitivity to shutdown corrosion when air was present in comparison to results obtained at Broadlands-Ohaaki when the pH was higher.

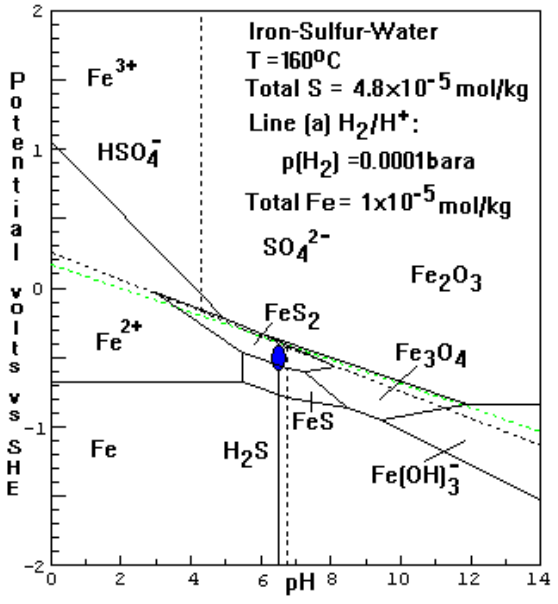

Figure 12. Moderate Gas Pourbaix diagram for steam at 160°C.

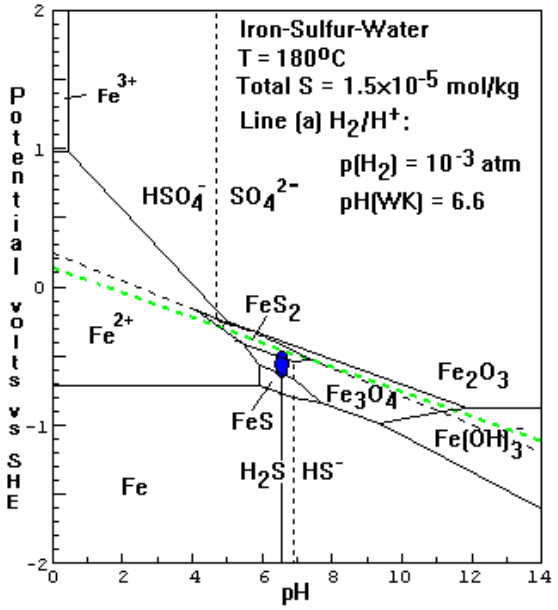

Figure 13. Low Gas Pourbaix diagram for steam at 180°C.

3. Separated steam tested during the high gas trials gave parabolic or logarithmic corrosion kinetics for all materials tested. The corrosion rates and local pit depths obtained were similar to those observed previously for 2.5 wt% gas in steam.

4. The Broadlands/Ohaaki well BR22 2.5 wt% gas database of materials test results can be used for high gas fluids with due recognition of the possibility of increased pitting and crevice corrosion under shutdown and startup conditions when fluids are subject to aeration.

ACKNOWLEDGEMENTS

The work reported here was sponsored by the New Zealand Government. The authors express their thanks to Quest Integrated for support and permission to publish this work.

REFERENCES

Arnorsson, S., Sigurdsson, S. and Svavarsson, H. (1982), The Chemistry of Geothermal waters in Iceland. Calculation of Aqueous Speciation from 0°C to 370°C, *Geochimica et Cosmochimica Acta*, **46**, 1513-1532.

Arnorsson, S. and Bjarnason, J.O. (1993) WATCH, Science Institure Orkustofnun, University of Iceland, Reykjavik, Iceland.

ASTM G1-03 (2003)Standard Practice for Preparing, Cleaning, and Evaluating Corrosion Test Specimens.

ASTM G4 – 01 (2008) Standard Guide for Conducting Corrosion Tests in Field Applications.

ASTM G46 – 94 (2005) Standard Guide for Examination and Evaluation of Pitting Corrosion.

ASTM G96 – 90 (2008) Standard Guide for Online Monitoring of Corrosion in Plant Equipment (Electrical and Electrochemical Methods).

Borshevsky M., Lichti K. A. and Wilson P. T. (1982) The Relationship between Corrosion Products and Corrosion Rates in Geothermal Steam, Pacific Geothermal Conference, November, pp 191-197.

Braithwaite, W.R. and Lichti, K.A. (1981) Surface Corrosion of Metals in Geothermal Fluids at Broadlands, New Zealand, ASTM STP 717, pp 81-112.

Chen, C.M., Arol, K. and Theas, G.J. (1983) Computer Calculated Potential pH Diagrams to 300°C, EPRI Report No. 3137.

Glover, R.B. (1982) Calculation of the Chemistry of Some Geothermal Environments, DSIR, Chemistry Division, Wairakei Report No. CD2323, March.

Glover, R.B. (1986) High Gas Trials Chemial Analysis Results and Calculation Ammendments, DSIR Chemistry Division Wairakei Letter, 2 April.

Henley, R.W. and Middendorf (1985) Geothermometry in the Recent Exploration of Mokai and Rotokawa Geothermal Fields, New Zealand in Geothermal Resources Council Trans, Vol 9, August, pp317-324.

Lichti, K.A. and Soylemezoglu, S. (1979) Geothermal Corrosion Monitoring Techniques, 1st New Zealand Geothermal Workshop, pp 233-238.

Lichti, K.A., Soylemezoglu, S. and Kunliffe, K.D. (1981) Geothermal Corrosion and Corrosion Products, 3rd New Zealand Geothermal Workshop, Auckland, New Zealand, pp 103-108.

Lichti, K.A. and Wilson, P.T. (1983) Materials Testing in Geothermal Steam, International Symposium on Solving Corrosion and scaling problems in Geothermal Systems, San Francisco, California, Jan 17-20, pp 269-284

Lichti, K.A., Driver, P.M., Wells, D.B. and Wilson, P.T. (1985) Mobile Corrosion Test Facility Commissioning Trials, Geothermal Steam 2.5wt% Gas, 7th New Zealand Geothermal Workshop, Auckland, pp 97-102.

Lichti, K.A., Driver, P.M., Caddie, B.J., Wells, D.B. Bijnan, H., Gould, T. and Wilson, P.T. (1991) Mobile Corrosion Test Facility High Gas Trials – 25wt% Gas, DSIR Internal Report No. RI3367.

Lichti, K.A., Wilson, P.T. and Inman, M.E. (1997) Corrosivity of Kawerau Geothermal Steam in Geothermal Resources Council Trans, Vol 21 Sept/Oct, pp 25-32.

Lichti, K.A., Bacon, L.G., (1998). Corrosion in Wairakei Steam Pipelines. 20th New Zealand Geothermal Workshop, Auckland, November, pp 51-58.

Lichti, K.A., Brown, K.L. and Ilao, C.M. (2000) Scaling and Corrosion of pH Adjusted Separated Water, 22nd New Zealand Geothermal Workshop, Auckland, Nov 8-10, pp 169-176.

Lichti, K. A., Klumpers, A. and Sanada, N. (2003) Utilisation of Acidic Geothermal Well Fluids Progress to 2002, 25th NZ Geothermal Workshop, pp 197-202.

Marshall, T. and Braithwaite, W.R. (1973) Corrosion Control in Geothermal Systems, Earth Sciences 12.

Plum, H. and Henley, R.W. (1983) Geothermal Fluid Chemistry at MK3 and MK4, Unpublished Results, Chemistry Division, Taupo, DSIR Technical Note 83/3 February.

Sheppard, D.S. and Giggenbach (1980) Chemistry of the Well Discharges at Ngawha, 2nd New Zealand Geothermal Workshop, pp 91-95.

Soylemezoglu, S., Lichti, K.A., Bijnen, H. (1980) Geothermal Corrosion Case Studies at Wairakei and Broadlands Geothermal Fields using the 'Corrosometer' Method, 2nd New Zealand Geothermal Workshop, Auckland, pp 27-31.

Wilson, P.T. and Lichti, K.A. (1982) Assessment of Corrosion Performance of Construction materials in Geothermal Steam, 4th New Zealand Geothermal Workshop, Auckland, pp 185-190.